CFD MODELING OF BLOOD FLOW INSIDE HUMAN LEFT CORONARY ARTERY BIFURCATION WITH ANEURYSMS

Nurullah Arslan*, Volkan Tuzcu**, Selman Nas**, Ayse Durukan*

*Fatih University, Graduate Institute of Sciences and Engineering, B. Çekmece, Istanbul, 34500, Turkey
**University of Arkansas for Medical Sciences, Department of Pediatrics, 800 Marshall Street, Little Rock, Arkansas, AR 72202, USA
*Fatih University, Industrial Engineering Department, B. Çekmece, Istanbul, 34500, Turkey

narslan@fatih.edu.tr, nasselman@uams.edu, tuzcuvolkan@uams.edu, aysedurukan@hotmail.com

Abstract:

Kawasaki disease (KD) affects primarily younger children and can lead to coronary artery aneurysms. The flow phenomena inside the left coronary artery and its branches with aneurysms located at various locations were studied computationally under steady flow conditions. Reynolds numbers representing the steady flow were 108, and 200 for average, and diastolic peak flow, respectively. Local arterial flow dynamics were analyzed inside the aneurysms with two different sizes (4 and 8 mm) located at the left main coronary artery (LCA) and at the left anterior descending (LAD) artery. The critical flow regions such as flow separation, flow recirculation inside the LCA and its branches were observed with changing magnitudes. These regions with disturbed laminar flow pattern may cause intimal hyperplasia inside the aneurysms and the bifurcation of the LCA. Disruption of the normal flow pattern may eventually lead to the formation of stenosis in the coronary artery. The rigidity due to the arterial thickening of the arteries may cause ischemia and even myocardial infarction in the end. Therefore, simulation of the flow patterns may provide us important information regarding the possible long-term implications of Kawasaki disease in children.

Introduction

Coronary aneurysm formation may occur in the acute stage of KD and this can lead to myocardial infarction and death [1, 2, 3], (Figure 1-A, B). Histopathologic and intravascular ultrasound studies have demonstrated marked thickening of the intimal layers of coronary arteries after KD [4, 5]. There is now evidence that flow-mediated endothelium-dependent vasodilatation is abnormal after KD [6–7]. KD was initially thought to be a benign self-limited childhood illness. However, soon after Kawasaki's original report [8], it became apparent that a few children diagnosed with KD died suddenly and unexpectedly, usually during the third or fourth week of illness and at a time when their clinical condition appeared to have improved. Death was usually due to massive myocardial infarction secondary to coronary thrombosis in areas of coronary artery aneurysm formation. About 20% of untreated KD patients develop coronary artery abnormalities, including diffuse peak frequency of coronary dilatation or dilatation and aneurysm formation. Hirose et al. demonstrated that coronary dilatation in patients with KD is first detected

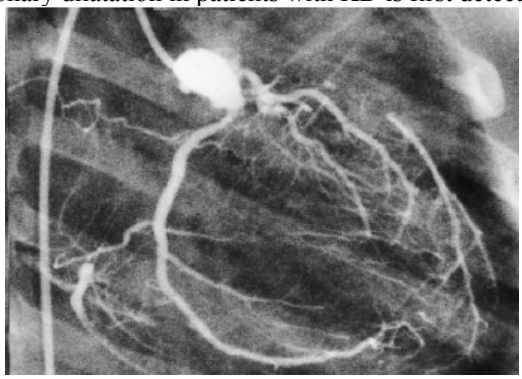

(A)

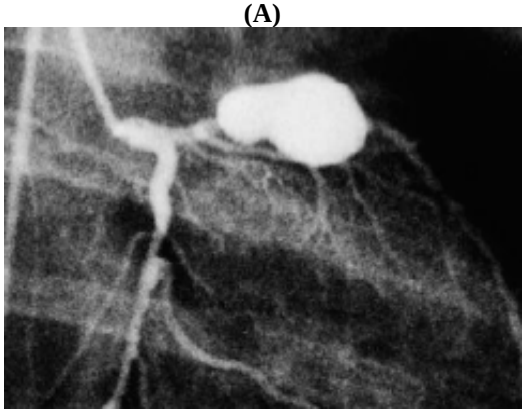

(B)

Figure 1: Coronary arteries with aneurysm located at the LCA artery (A) and at the LAD artery (B)

at a mean of 10 days of illness and that the peak frequency of coronary dilatation or aneurysms occurs within 4 weeks of onset [9]. Thus, KD is an acute vasculitis; there is no evidence of chronic, ongoing vasculitic changes in the arterial wall of the KD patient whose acute illness has resolved. Saccular and fusiform aneurysms usually develop between 18 and 25 days after the onset of illness. The fatality rate in KD is dependent upon prompt recognition of cases and institution of appropriate therapy. Initial reports from

*Corresponding author, Tel: +90 212 889 0837 Fax: +90 212 889 1142
E-mail: narslan@fatih.edu.tr

ISSN: 1727-1983

Japan in the 1970s indicated a 1 to 2% fatality rate; this has dropped to 0.08% [10] due to improved recognition and therapy of the disorder. Recently, fatality rates of 6% from Auckland [11], 2% from Sweden [12], and 3.7% from the British Isles [13] were reported. Death in these series was due either to myocardial infarction secondary to thrombosis of a coronary artery aneurysm or to rupture of a large coronary artery aneurysm. Death is most common 2 to 12 weeks after the onset of illness. The fate of coronary aneurysms over time was well described by Kato et al. [14]. At 1 to 3 months after the onset of KD, 15% of KD patients in this study had angiographic evidence of coronary artery aneurysms. Repeat angiography 5 to 18 months later in those with abnormalities showed that the aneurysms had resolved in about 50% of the patients. Of those with persistent aneurysms, one-half had smaller aneurysms than previously, with or without stenosis, one-third had resolution of the aneurysms but had developed obstruction or stenosis of the coronary arteries, and the remainder had fine irregularities of the vessel walls without stenosis. Stenosis, which occurs as a result of the healing process of the vessel wall, often leads to significant coronary obstruction and myocardial ischemia. A recent longer-term follow-up study by Kato et al. indicated that 10 to 21 years after acute KD, additional patients with persistent aneurysms had developed stenosis of the vessel [14]. Myocardial infarction occurred in 39% of patients with persistent aneurysms with stenosis, or 1.9% of all the KD patients in this series. Bypass surgery was performed in 1.2% of all KD patients, or 25% of patients with persistent aneurysms with stenosis. The overall mortality in this group of 594 patients was 0.8% [15]. The most severe form of coronary artery aneurysm is the giant aneurysm (internal luminal diameter of the coronary artery lumen, ≥8 mm). These lesions are less likely to resolve and more likely to thrombose, rupture, or eventually develop stenosis than other, smaller aneurysms [16]. In the long-term follow-up study by Kato et al. 26 of 594 patients (4.4%) developed giant coronary aneurysms [17]; in 12 of the 26 patients (46%), stenosis or complete obstruction occurred over time, and 8 of the 12 (67%) experienced a myocardial infarction, with a 50% mortality rate. The other 14 patients showed persistent coronary aneurysms without stenosis over the 10 to 21-year follow-up period. KD results in vasculitis of the large to medium-sized arteries; weakening of the arterial wall leads to dilatation and aneurysm formation. Some patients experience mild vasculitis, which is insufficient to cause weakening of the wall of the coronary artery; the long-term consequences of this less severe vasculitis is unknown. The vasculitis of KD also may affect other noncoronary medium-sized arteries throughout the body. Systemic artery aneurysms occur in about 2% of patients, generally in those who also have coronary artery aneurysms [18]. The most commonly affected arteries are the renal, paraovarian or paratesticular, mesenteric, pancreatic, iliac, hepatic, splenic, and axillary arteries [19, 20]. Since arteritis in these vessels is less likely to be the cause of death in KD than is coronary arteritis, this complication has received less attention. It is likely that vasculitis without aneurysm formation occurs in many vessels in KD patients with coronary disease; the true extent of the vasculitis is probably apparent only at autopsy [21]. Flow-mediated dilatation in experimental models depends on the ability of the endothelium to release nitric oxide in response to shear stresses. The flow field analysis was done inside the arterivenous graft to vein connections, bypass connections and aneursmys to understand the effect of critical flow regions on the endothelial cells, [22, 23, 24, 25, 26]. In this study the critical flow regions such as flow separation regions, stagnation regions and flow recirculations regions inside the LCA, circumflex artery, and LAD artery with aneursym located at the left main coronary artery and LAD artery was investigated to understand if the abnormal flow behaviour can cause the formation of stenosis and the rupture of the aneursyms located on the local arteries.

Methods

Aneuryms were created on the basis of images supplied by the cardiac surgeons representing the typical alternative designs, Figure 1-A, B, [3]. 3-D models of typical coronery arteries with the aneurysm located at the LCA and LAD artery shown in Figure 2 were utilized using ACIS-based solid modeller Gambit (Fluent Inc., Lebanon, NH, USA) where the 3-D model and mesh were also created. The diameters of the aneurysms were changed to investigate the effects of the geometry on the local flow dynamics inside the models. Two different geometries with the diameters changing from four to eight millimeters in diameters from each configuration were used. Two geometries are made with an entrance artery and two branching arteries connected to the entrance artery. The diameter of the entrance artery and branching arteries were taken as three millimeters in diameters. All models were meshed with an automatic meshing algorithm using tetrahedral elements.

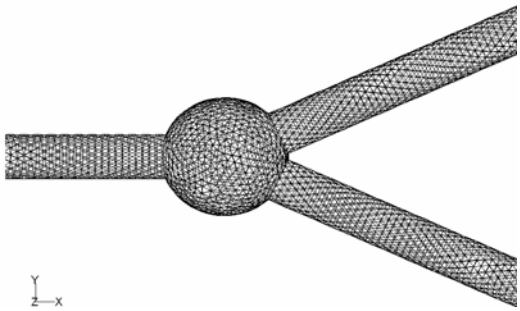

(A)

ISSN: 1727-1983

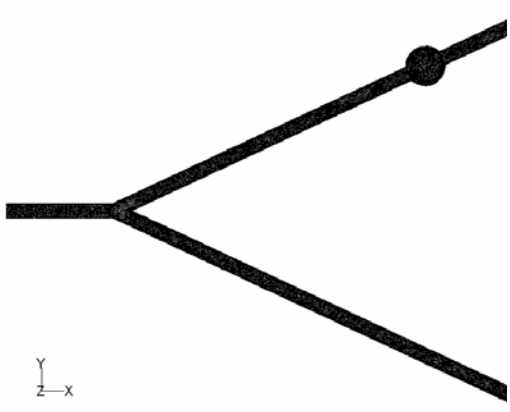

(B)

Figure 2: Aneursyms models located at the LCA artery and LAD artery used for the computational calculations

Boundary Conditions and Simulations

The commercial finite volume code Fluent, Fluent Inc., Lebanon, NH, USA was used in this study. A segregated solver was selected and convergence criteria was selected as 10^{-8}. All models were meshed with an automatic meshing algorithm using tetrahedral elements. Vessel walls were assumed to be rigid and impermeable. Blood was assumed to behave like a Newtonian fluid with a constant density ρ=1050 kg/m^3 and dynamic viscosity μ=0.0035 kg/m.s. The models were submitted to steady flows. Since the LCA is quite short leading to entrance type flow, the inlet velocity profile was selected as flat velocity profile at the entrance and developed to the parabolic velocity profile. The entrance velocities were selected as 0.14 m/s at average, and 0.25 m/s at diastolic flow, respectively. The Reynolds numbers based on the inlet diameter (Re = ρUD/ μ, where ρ: fluid density, U: Inlet velocity, D: Inlet diameter, μ: dynamic viscosity) at the diastolic peak and mean flow were 200 and 108, respectively. The flow distribution rates were assumed to be 70 % leaving from the left anterior descending and 30 % leaving from left circumflex artery, [26]. The flow distribution rate was defined as FR= (Q_{outlet} / Q_{inlet}) $\times$100% where Q_{outlet} is the mean flow in one of the outlet coroner arteries either left circumflex artery (LCX), or LAD artery and Q_{inlet} is inlet mean flow rate. Simulations were performed on a Pentium (R) 4 CPU 2.800 GHz with 1,024 MB of RAM.

Results and Discussion

The detailed investigation of the flow patterns inside the LCA, LCX and the LAD arteries with aneursyms were investigated. Two different models were: (1) aneursym located at the LCA and (2) aneursym located at the LAD artery. The flow velocity profiles for two different diameters of aneursyms located at the LCA were given in Figure 3, A-B at Reynolds nuımber of 108 and Figure 4, A-B, at Reynolds number of 200. We can readily observe that significant secondary motion prevails in the large size aneursyms. The intensities of the secondary

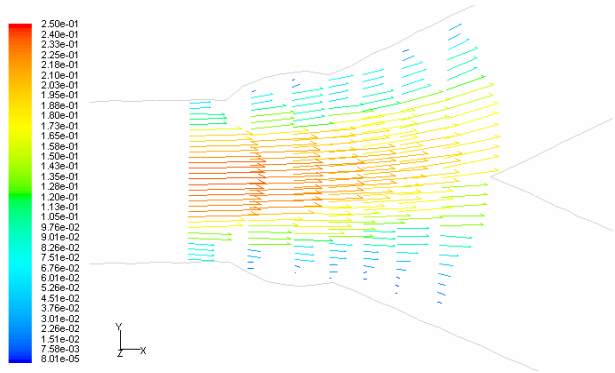

(A)

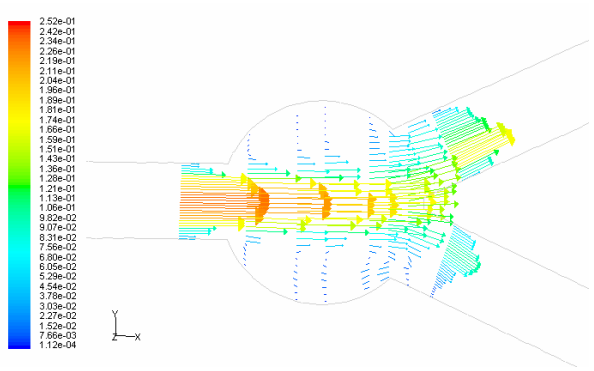

(B)

Figure 3: A and B, Velocity profiles inside the aneursym located at the LCA artery, D = 4mm and 8mm, Re = 108

the flow increased from mean phase to the diastolic peak. The inflow-outflow patterns observed.

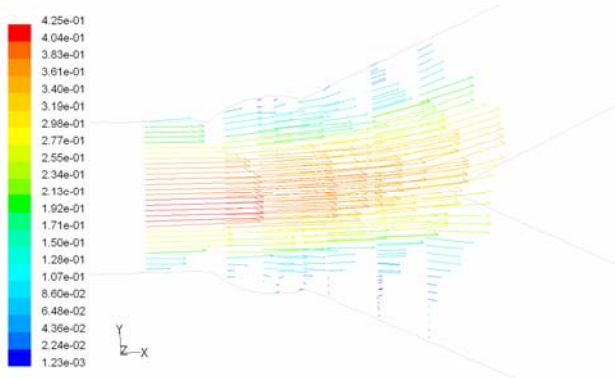

(A)

ISSN: 1727-1983

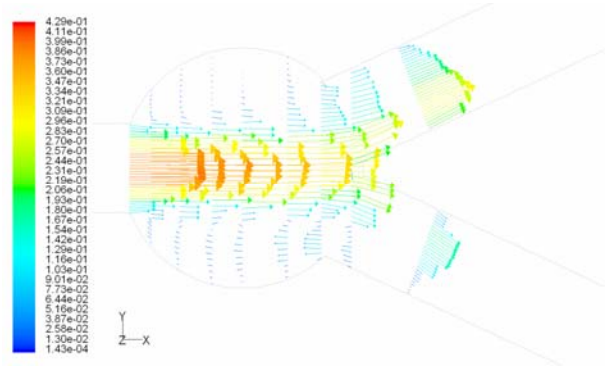

(B)

Figure 4: A and B, Velocity profiles inside the aneursym located at the LCA artery, D = 4mm and 8mm, Re = 200

Aneurysm located at the LCA

Average Flow(Re=108) and Diastolic Phase (Re=200)

The flow velocity profiles for two different aneursyms were shown in Figure 3, 4. Velocity profile was flat at the inlet of the main coronary artery and developed to the parabolic velocity profile through the main coronary artery which is similar to the flow inside the straight pipe flow, Poiseuille flow. When the diameter of the aneursysm was four millimeters, the flow was smooth inside the aneursym located at the main trunck, Figure 3, A-B. There was a weak sudden expansion at the entrance of the aneursym. Then the flow was divided into two branches, LCX and LAD arteries. Separation region formed after the flow exiting the aneursym at the entrance of the LCX artery. The size of the separation region was approximately one diameter of the inlet diameter, Figure 3, A. While the diameter of the aneursym increases the flow pattern inside them becomes more complex. Separation bubbles were formed which will cause the lower wall shear stresses inside the aneursyms, Figure 3-B and 4-B. Strong separation region also found at the outlet of the aneursym. These separation regions were combined with the separation formed at the entrance of the LCX artery. No separation region were formed at the inlet of the LAD arteries. Figure 3 illustrates the velocity profiles that illustrate a strong reverse wall shear stress (WSS) at the corners opposite to the flow divider. A complex set of interacting vortices is produced in each branch from the compound curvatures. The secondary flows do not become pronounced until several diameters of the bifurcation. The low momentum of fluid at the outer walls of the bifurcation causes fluid to oscillate in direction during cardiac cycle. When the diameter of aneursym was increased to the eight millimeters, the results are characterized by a jet of fluid passing directly through the aneursym surrounded by an annular recirculating vortex, Figure 3-B and 4-B. Separation occurred inside the aneursym. The flow was rotational inside the aneursym. Velocities of the fluid particles near the wall were slow causing the low WSS, Figure 3-B and 4-B. Flow was compressed through the exit of the aneursym. Then the flow was exited after the aneursym and divided into two branches, LCX and LAD arteries. There was separation region on circumflex artery . The size of the separation region was one diameters of the inlet diameter. The stagnation point was detected at the location of one and a half length of inlet diameter after the the flow division on the side of circumflex artery. The flow then continued similar to the flow seen in the diameter of four millimeters. At the diameter of eight millimeter, strong double vortex was seen inside the aneursym and this vortex was transported to the arterial bifurcation through the LCX artery, Figure 3-B and 4-B. During the diastolic phase the flow structure inside the aneursym and the LAD artery and LCX artery stayed same. However the velocity magnitude became higher, Figure 3-B and 4-B..

Aneurysm located at the LAD artery

Average Flow(Re=108) and Diastolic Phase (Re=200)

The flow entered the LCA artery with a flat velocity profile and developed to the parabolic velocity profile until it reaches to the bifurcating point. The flow was divided to two branches as the LCX and LAD arteries. The velocity profiles are strongly skewed at the flow divider. Figure 5-A illustrates the velocity profiles that illustrate a strong reverse wall shear stress at the corners opposite the flow divider. A complex set of interacting vortices is produced in each branch from the compound curvatures. Then the flow entered to the aneursym at the location of twenty inlet diameter downstream of the flow after bifurcation point located at the LAD artery illustrated in Figure 5-B. For the current study, no aneursyms were assumed to locate along the LCX artery. Two aneursyms with diameters of four millimeters and eight millimeters were considered to investigate the effect of the geometry on the flow rates and the flow structure. There was a weak secondary flow inside the aneursym at diameter of four millimeters. The flow was similar to the flow inside the straight pipe flow after exiting from aneursym. When the diameter of the aneursym became eight millimeters, the flow in the bifurcation region was similar to the one mentioned before, four millimeter. The flow was rotational inside the aneursym. Double vortexes were formed inside aneursym, Figure 6-B.

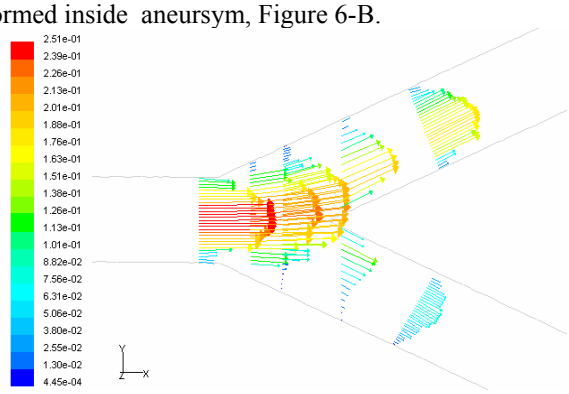

(A)

ISSN: 1727-1983

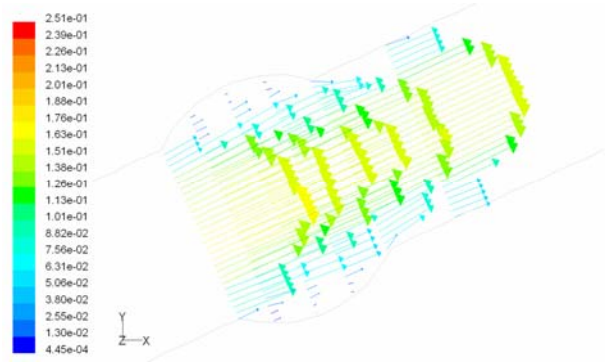

(B)

Figure 5: Velocity profiles at the branch of LCX and LDA and inside the aneursym located at LAD artery, D = 4mm Re = 108

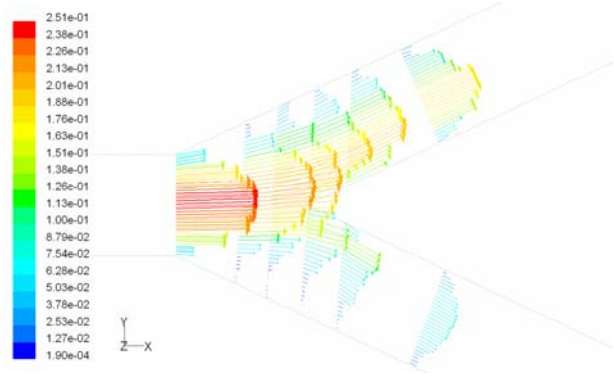

(A)

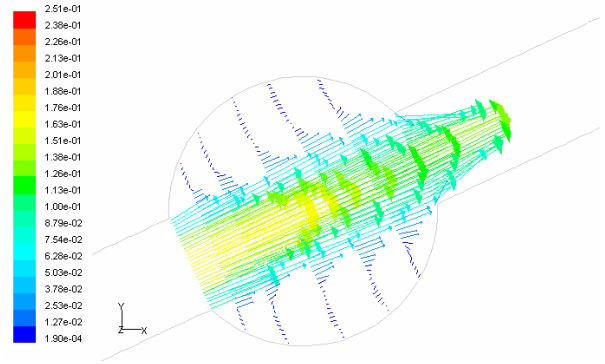

(B)

Figure 6: Velocity profiles at the branch of LCX and LDA and inside the aneursym located at LAD artery, D = 8mm Re = 108

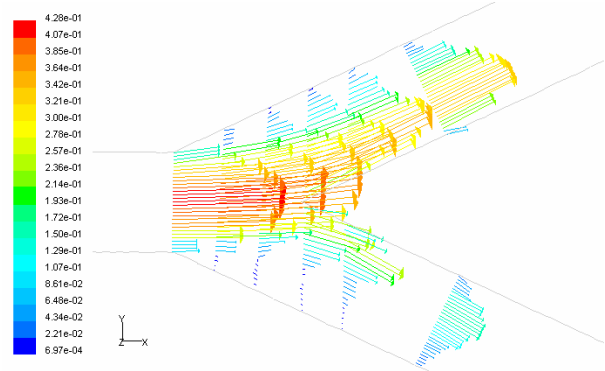

(A)

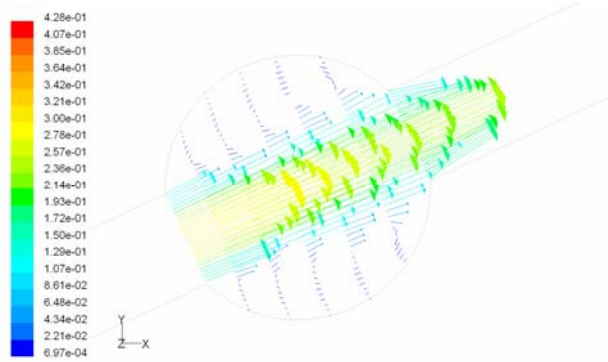

(B)

Figure 7: Velocity profiles at the branch of LCX and LDA and inside the aneursym located at LAD artery, D = 8mm Re = 200

Conclusions

Hemodynamics inside the aneurysms located at the LCA followed by the LCX artery and LAD artery was investigated computationaly. The principal findings of this study is that both of the aneurysms are parallel to the main flow and behave like a driven cavity. The recirculation fluid region was formed inside the aneursyms at the diameter of eight millimeter but four millimeter. The strong secondary flow was detected inside both aneursysms with the changing diameters of four to eight millimeters. There are also secondary flows occurring at the inlet of LCX and LAD arteries. The effect of the size of aneursyms on the exit flow ratios was also studied and the flow reduction on the branch which has the aneursym was located. This study is driven by the need to establish a technique that can identify the optimum regions for coil embolization. We conclude that this identification can benefit greatly from simulations of the nature performed herewith based on the observations made. Such optimum embolization regions seem to be strongly connected not only with patient-specific but also with aneursym-specific hemodynamics and thus insight on this kind of individual-based blood flow data can prove valuable for advanced intervention techniques. Future studies will focus on the clinical studies and also the experimental modeling studies to understand the flow field better with the higher spatial resolution.

Acknowledgements

The authors would like to thank cardiac surgeon Soichiro Kitamura from National Cardiovascular Center in Osaka, Japan sending his research images to be used in this study.

References

[1] Kawasaki T, Kosaki F, Okawa S, Shigematsu I, Yanakawa S., (1974): 'A new infantile acute febrile mucocutaneous lymph node syndrome

(MLNS) prevailing in Japan', Pediatrics;54: 271–6.

[2] Kato H, Ichinose E, Kawasaki T. (1986): 'Myocardial infarction in Kawasaki disease: clinical analyses in 195 cases', J Pediatr;108:923–7.

[3] Kitamura, Soichiro, (2002): 'The role of coronary bypass operation on children with Kawasaki disease. Coronary Artery Disease', Vol 13 No 8:437-447

[4] Tanaka N, Naoe S, Masuda H, Ueno T., (1986): 'Pathological study of sequelae of Kawasaki disease (MCLS): with special reference to the heart and coronary arterial lesions', Acta Pathol Jpn;36:1513–27.

[5] Suzuki A, Yamagishi M, Kimura K, (1996):. 'Functional behavior and morphology of the coronary artery wall in patients with Kawasaki disease assessed by intravascular ultrasound', J Am Coll Cardiol;27:291–6.

[6] Yamakawa R, Ishii M, Sugimura T, (1998):. 'Coronary endothelial dysfunction after Kawasaki disease: evaluation by intravascular injection of acetylcholine', J Am Coll Cardiol; 31:1074–80.

[7] Mitani Y, Okuda Y, Shimpo H, (1997): 'Impaired endothelial function in epicardial coronary arteries after Kawasaki dis-ease', Circulation;96:454–61.

[8] Kawasaki T., (1967): 'Pediatric acute febrile mucocutaneous lymphnode syndrome with characteristic desquamation of fingers and toes: my clinical observation of 50 cases [in Japanese]'. Jpn J Allergol;16:178–222. Translation by H Shike, C Shimizu, JC Burns [online 2002]. Available at http//www.pidj.com.

[9] Hirose, O., H. Misawa, Y. Kijima, O. Yamada, Y. Arakaki, Y. Kajino, Y. Ryujin, T. Kowata, S. Echigo, and T. Kamiya. (1981): 'Two dimensional echocardiography of coronary artery in Kawasaki disease (MCLS): detection, changes in acute phase, and follow-up observation of the aneurysm', J. Cardiogr. 11:89–104. (In Japanese with English abstract.)

[10] Yanagawa, H., Y. Nakamura, M. Yashiro, T. Ojima, H. Koyanagi, and T. Kawasaki. (1996): 'Update of the epidemiology of Kawasaki disease in Japan from the results of the 1993–1994 Nationwide survey', J. Epidemiol. 6:148–157.

[11] Gentles, T. L., P. M. ClarKDon, A. A. Trenholme, D. R. Lennon, and J. M. Neutze. (1990): 'Kawasaki disease in Auckland, 1979–1988', N. Z. Med. J. 103: 389–391.

[12] Schiller, B., A. Fasth, G. Bjorkhem, and G. Elinder. (1995): 'Kawasaki disease in Sweden: incidence and clinical features', Acta Pediatr. 84:769–774.

[13] Kato, H., E. Ichinose, F. Yoshioka, T. Takechi, S. Matsunaga, K. Suzuki, and N. Rikitake. (1982). 'Fate of coronary aneurysms in Kawasaki disease:serial coronary angiography and long-term follow-up study', Am. J. Cardiol.49:1758–1766.

[14] Kato, H., T. Sugimura, T. Akagi, N. Sato, K. Hashino, Y. Maeno, T. Kazue, G. Eto, and R. Yamakawa. (1996):, 'Long-term consequences of Kawasaki disease', Circulation 94:1279–1285.

[15] Nakano, H., K. Ueda, A. Saito, and K. Nojima. (1985):, Repeated quantitativeangiograms in coronary arterial aneurysm in Kawasaki disease. Am. J. Cardiol. 56:846–851.

[16] Akagi, T., H. Kato, O. Inoue, N. Sato, and K. Imamura. (1990). Valvular heart disease in Kawasaki syndrome: incidence and natural history. Am. Heart J. 120:366–372.

[17] Kato, H., O. Inoue, and T. Akagi. (1988): 'Kawasaki disease: cardiac problems and management', Pediatr. Rev. 9:209–217.

[18] Sigamura, T., H. Kato, O. Inoue, T. Fukuda, N. Sato, M. Ishii, J. Takagi, T. Akagi, Y. Maeno, T. Kawano, T. Takagishi, and Y. Sasaguri. 1994. Intra-Vol. 11, (1998): 'Kawasaki Syndrome 413 vascular ultrasound of coronary arteries in children. Assessment of the wallmorphology and the lumen after Kawasaki disease', Circulation 89:258–265.

[19] Suzuki, A., M. Yamagishi, K. Kimura, H. Sugiyama, Y. Arakaki, T. Kamiya, and K. Miyatake. (1996):, 'Functional behavior and morphology of the coronary artery wall in patients with Kawasaki disease assessed by intravascular ultrasound' J. Am. Coll. Cardiol. 27:291–296.

[20] Burns, J. C., H. Shike, J. B. Gordon, A. Malhotra, M. Schoenwetter, and T. Kawasaki. (1996):, 'Sequelae of Kawasaki disease in adolescents and young adults' J. Am. Coll. Cardiol. 28:253–257.

[21] Kato, H., O. Inoue, T. Kawasaki, H. Fujiwara, T. Watanabe, and H. Toshima. (1992):, 'Adult coronary artery disease probably due to childhood Kawasaki disease'. Lancet 340:1127–1129.

[22] Arslan N. (1999):, 'Experimental haracterization of transitional unsteady flow inside a graft-to-vein junction', Ph.D. thesis, The University ofIllinois at Chicago.

[23] Loth F., Fischer P.F., Arslan N., Bertram C.D., Lee S.E., Royston T.J., Song R.H., Shaalan W.E., Bassiouny H.S. (2003):, 'Transitional flow at the venous anastomosis of an arteriovenous graft: Potential activation of the ERK1/2 mechanotransduction pathway', J. Biomech. Engrg. 125 49–61.

[24] Arslan N., Loth F., Bertram C.D., Bassiouny H.S. (2005):, 'Transitional flow field characterization inside an arteriovenousgraft-to-vein anastomosis under pulsatile flow

ISSN: 1727-1983

conditions', European Journal of Mechanics B/Fluids 24(3) 353–365 May-June

[25] Giddens D.P., Zarins C.K., Glagov S. (1990):, Response of arteries to near-wall fluid dynamics behavior, Appl. Mech. Rev. 43 S98–S102.

[26] Boutsianis, E, dave H., Fraunfelder T, Poulikakos D., Wildermuth S, Turina M, Ventikos Y, Zund G, (2004):'Computational simulation of intracoronary flow based on real coronary geometry', European Journal of cardiothoracic Surgery, 26, 248-256

ISSN: 1727-1983